γ

BNL 37364

BNL--37364

DE86 005678

Λ and Σ HYPERNUCLEI

D. J. Millener

Brookhaven National Laboratory**

Upton, New York 11973

*Invited talk at the International Symposium on Hypernuclear and Kaon Physics, Brookhaven; September 9-13, 1985

DISCLAIMER

Λ and Σ HYPERNUCLEI

D. J. MILLENER

Brookhaven National Laboratory
Upton, New York, USA 11973

The present status of structure calculations for p-shell Λ hypernuclei, including the phenomenological determination of ΛN effective interaction matrix elements, is briefly reviewed. For Σ hypernuclei the Nijmegen potential model D is used for guidance in constructing ΣN effective interactions. The structure of ${}^{12}_{\Sigma}$Be and ${}^{12}_{\Sigma}$C, including isospin mixing in the latter case, is discussed, and a comparison is made with experimental data.

1. Λ HYPERNUCLEI

The structure of p-shell Λ hypernuclei appears to be quite well understood in the sense that shell-model calculations using phenomenological ΛN effective interactions can satisfactorily account for the measured excitation energies and spins[1,2]. For a lambda in the lowest s orbit the spectra are determined by the $p_N s_\Lambda$ two-body interaction which can be characterized[2] in terms of five radial integrals. These are conventionally denoted by $\bar{V}$, Δ, S_Λ, S_N and T, and are associated with the radial dependence of the operators 1, $S_N \cdot S_\Lambda$, $\ell_{N\Lambda} \cdot S_\Lambda$, $\ell_{N\Lambda} \cdot S_N$ and S_{12}. The splitting of doublets based on core levels of non-zero spin depends on Δ, S_Λ and T, while S_N can affect the separation of states based on different core levels. $\bar{V}$ enters only into the binding energy, where a three-body ΛNN interaction seems necessary[2,3] to reproduce the smooth behaviour of the Λ separation energies as a function of A.

The spin dependence of the ΛN interaction required to fit energies of excited states, deduced from the energies of observed γ-rays, can be compared[2] with that deduced from the Nijmegen ΛN interaction[4]. The calculated non-central matrix elements are small in agreement with data, especially for the Λ spin-orbit interaction. However, in the case of the central interaction, the singlet interaction is found to be stronger than the triplet, in contrast to the free ΛN interaction. The effective $p_N S_\Lambda$ interaction is consistent with an earlier interaction[1] which worked well for $p^n p_\Lambda$ states observed in (K^-,π^-) reactions.

The cross sections for the formation of Λ hypernuclear states in (K^-,π^-) reactions are well understood[1] in terms of the distorted wave Born

approximation. The essential ingredients are the use of distorted waves obtained from fits to elastic scattering data for kaons and pions, the strength of the Fermi-averaged elementary $K^-n \to \pi^-\Lambda$ forward amplitudes and the structure information contained in the one-body density matrix elements from the shell-model calculations.

2. Σ HYPERNUCLEI

Data from CERN, BNL and KEK exist for a number of p-shell targets from ^{6}Li to ^{16}O and for incident momenta between 400 MeV/c and 720 MeV/c. In most instances the statistics are rather poor, and the candidates for Σ-hypernuclear lines are often not easily distinguished from the background. The backgrounds, due in part to broad Σ-hypernuclear excitations and also to the quasi-elastic process, are uncertain. The theory too is beset with many uncertainties, aside from limited knowledge of the ΣN interaction. For example, our shell-model and DWBA calculations do not take into account the unbound nature of the observed Σ-hypernuclear excitations. Consequently, we are often reduced to looking for a certain degree of consistency between the theoretical predictions and the available data. It should be emphasized that the narrow peaks observed so far, with the exception[5] of a peak in $^{6}_{\Sigma}$H, appear to correspond to Σ particles produced in unbound p orbits and that the relatively small widths of the states are not fully understood.

2.1 QUASI-ELASTIC TRANSITIONS

In the Fermi gas model one finds[6] an approximately parabolic shape for the quasi-elastic contribution to the $^{A}Z\ (K^-,\pi^+)\ ^{A}_{\Sigma}(Z-2)$ cross section centered at $\omega = M_{HY} - M_A$ given by

$$\bar{\omega} = m_{\Sigma^-} - m_p + U_p - U_{\Sigma^-} - \left(\frac{1}{m_p} - \frac{1}{m_{\Sigma^-}}\right)\frac{k_F^2}{4} + q^2/2m_{\Sigma^-}$$

with a full width a half maximum $\Gamma_{1/2} = \sqrt{2}\, qk_F/m_{\Sigma^-}$.
Both $\Gamma_{1/2}$ and $\bar{\omega}$ increase with q; at 0°

$$q^2/2m_{\Sigma^-} = \begin{cases} 1 \text{ MeV (400 MeV/c)} \\ 1.7 \text{ MeV (450 MeV/c)} \\ 3.4 \text{ MeV (550 MeV/c)} \\ 6.5 \text{ MeV (713 MeV/c)} \\ 12.1 \text{ MeV (at rest)} \end{cases}$$

where the K^- lab momentum is given in parentheses.

A good candidate for a quasi-elastic peak is the broad bump ($\Gamma_{1/2} \approx 20$ MeV) seen[5] in the ^{16}O (K^-,π^+) $^{16}_{\Sigma}$C spectrum at 713 MeV/c. From the peak position, $\bar{\omega} = 286$ MeV, a value for $U_p - U_{\Sigma^-}$ of 24.6 MeV can be extracted. After taking out the Coulomb contributions to U_p and U_Σ the strong Σ^- potential turns out to be slightly weaker than the Λ potential, a result consistent with that extrac-

ted from analyses of Σ^- atomic data[7]. Using the above value for $U_p - U_{\Sigma^-}$ one can now predict the energy of the quasi-elastic peak for other incident momenta. For example

$$\bar{\omega} = \begin{cases} 281.2 \text{ MeV for } ^{12}C\ (K^-,\pi^+)\ ^{12}_{\Sigma}Be \text{ at } 450 \text{ MeV/c} \\ \quad \text{or for } ^{16}O\ (K^-,\pi^+)\ ^{16}_{\Sigma}C \text{ at } 450 \text{ MeV/c} \\ 291.6 \text{ MeV for } ^{12}C\ (K^-,\pi^+)\ ^{12}_{\Sigma}Be \text{ at rest} \end{cases}$$

The value of $\bar{\omega}$ at rest is consistent with the quasifree background assumed by Yamazaki et al[8], while the value for p_K = 450 MeV/c puts a broad quasi-elastic contribution in the region where narrow structure has been observed[9,10], thus complicating the extraction of cross sections or even relative intensities for narrow peaks.

2.2 ΣN TWO-BODY MATRIX ELEMENTS

To discuss the structure seen in recent $(K^-,\pi^\pm)$ reactions[8,9,10] on ^{12}C and ^{16}O targets we need ΣN two-body matrix elements for $p_N p_\Sigma$. We follow the procedure used for ΛN interactions[2] and obtain $p_N s_\Sigma$ matrix elements by cutting off the model D potential of the Nijmegen group[4] inside a radius r_0. The result, for r_0 = 1.2 fm, is shown in Table 1 where a comparison is made with our standard set[2] of $p_N s_\Lambda$ two-body matrix elements.

Table 1

	$p_N s_Y$ Matrix Elements[a]		
	ΛN T=1/2	ΣN T=1/2	ΣN T=3/2
V^s	-1.87	-0.37	-3.06
V^t	-1.37	-2.22	-0.76
S_Y	-0.04	-0.04	-0.06
S_N	-0.08	-0.03	-0.08
T	0.04	-0.43	0.21

[a]Based on model D of Ref. 4 with r_0 = 1.2 fm. Note that $-V^t = \bar{V} - 1/4\ \Delta$ and $-V^s = V + 3/4\ \Delta$ for V and Δ defined as in Ref. 2.

We notice that the central interaction exhibits a strong spin-isospin dependence with the strongest attraction being in the triplet channel for T=1/2 and in the singlet channel for T=3/2. The spin orbit interactions are weak, only slightly stronger than for ΛN. The tensor matrix elements are quite large and exhibit a clear $t_N \cdot t_\Sigma$ dependence associated with pion exchange. One other feature of the model D ΣN interaction is that space exchange components are very weak.

We obtain central and tensor matrix elements for $p_N p_\Sigma$ by choosing the strengths of Yukawa interactions in each channel to reproduce the $p_N s_\Sigma$ matrix elements of Table 1. The range of the Yukawa interaction then fixes the ratio

$F^{(2)}/F^{(0)}$ which characterizes p-shell effective interactions[1]. We replace the spin-orbit interactions by an effective one-body spin-orbit interaction characterized by the parameter $\epsilon_p = \epsilon_{p1/2} - \epsilon_{p3/2}$. The only essential complication with respect to the case of Λ hypernuclei[1] arises because Σ^- and Σ^0 are 7.98 and 4.88 MeV respectively heavier than Σ^+. These mass differences are not fully compensated for by the corresponding Coulomb energies so that in general Σ-hypernuclear states will not have good isospin. For the Coulomb energy of Σ with respect to a core we use $V_c = Z_{core} \cdot C \cdot m_{t_\Sigma}$. Then C = 0.57 MeV if we take, e.g., the value V_c = 2.8 MeV for A=12 estimated by Batty, Gal and Toker[11].

2.3 THE A = 12 Σ HYPERNUCLEI

The $^{12}C(K^-,\pi^+)^{12}_{\Sigma}Be$ reaction[9] at p_K = 450 MeV/c shows a peak of width 4±1 MeV at $M_{HY}-M_A$ = 279 MeV followed by a broad shoulder at higher excitation energy. Since $p_N \to p_\Sigma$ ΔL=0 transitions are strongly favored at the forward angle of this experiment, the peak has been interpreted in terms of the ^{11}B gs × $p_{3/2\Sigma}$ 0^+ configuration. The spectrum observed at the larger momentum transfer of the $^{12}C(K^-,\pi^-)^{12}_{\Sigma}Be$ reaction with stopped kaons[8] is qualitatively different. Two, and possibly three, peaks have been observed, and the splitting of 4.6±0.6 MeV between the peaks at $M_{HY}-M_A$ = 277.2±0.3 MeV and 281.8±0.5 MeV has been attributed largely to a spin-orbit splitting of the $p_{3/2}$ and $p_{1/2}$ Σ^- orbitals. The rationale for this interpretation can be seen from the pure weak-coupling results displayed in Table 2.

Table 2

$^{12}_{\Sigma}Be$ in the weak-coupling limit for ϵ_p = 5 MeV

E_x(MeV)	Configuration	J^π	$\rho^2(\Delta S=0)$	$d\sigma/d\Omega$(rel.)
0	$3/2^-_1 \times p_{3/2\Sigma}$	0^+	0.475	1
		2^+	0.237	
2	$1/2^-_1 \times p_{3/2\Sigma}$	2^+	0.126	
5	$3/2^-_1 \times p_{1/2\Sigma}$	2^+	0.237	0.40
	$3/2^-_2 \times p_{3/2\Sigma}$	0^+	0.063	
		2^+	0.032	
7	$1/2^-_1 \times p_{1/2\Sigma}$	0^+	0.126	0.15

In Table 2

$$\rho^2(\Delta S=0) = \frac{S}{2(2j_N+1)} \begin{pmatrix} 1 & 1/2 & j_\Lambda \\ 1 & 1/2 & j_N \\ \Delta L & 0 & \Delta L \end{pmatrix}^2 ,$$

where S = 5.70, 1.51, and 0.76 for the gs, 2.12 MeV and 5.02 MeV levels of ^{11}B respectively. In obtaining relative cross sections the result of Gal and Klieb[12] that 0^+ is favored over 2^+ in the ratio 0.57:0.43 has been used. The existence of the lower two peaks including their ratio[8], but not a third peak, can be explained for ϵ_p = 5 MeV.

Table 3

ΣN effective interactions

Interaction[a]	T = 1/2		T = 3/2			
	V^t	V^s	V^t	V^s	μ(fm)	$\bar{F}^{(0)}$
G1	-29.0	-8.8	-10.8	-45.0	1.0	-1.03
G3	-29.0	0.0	0.0	-45.0	1.0	-0.73
M1	-90.0	-30.0	-22.5	-90.0	0.7	-1.03
M2	-94.7	-15.8	-14.3	-114.6	0.7	-1.03
M3	-100.0	0.0	0.0	-157.5	0.7	-1.03
M4	-50.0	-50.0	-50.0	-50.0	0.7	-1.00

[a]Yukawa forms, strengths in MeV. $F^{(2)}/F^{(0)}$ = 2.43, 3.07 for μ = 1.0,0.7. All interactions except M4 contain a tensor force of range μ=1 fm with V(T=1/2) = -52.0 and V(T=3/2) = 25.0.

We now study the effects of the ΣN interaction, several of which are listed in Table 3. Fig. 1 shows the distribution of formation strength, in the form $\rho^2(\Delta S=0)$, as a function of ϵ_p for the interaction M4 which is central, spin and isospin independent, and similar to the ΛN effective interaction. For ϵ_p small there is a strong tendency to concentrate the formation strength in a

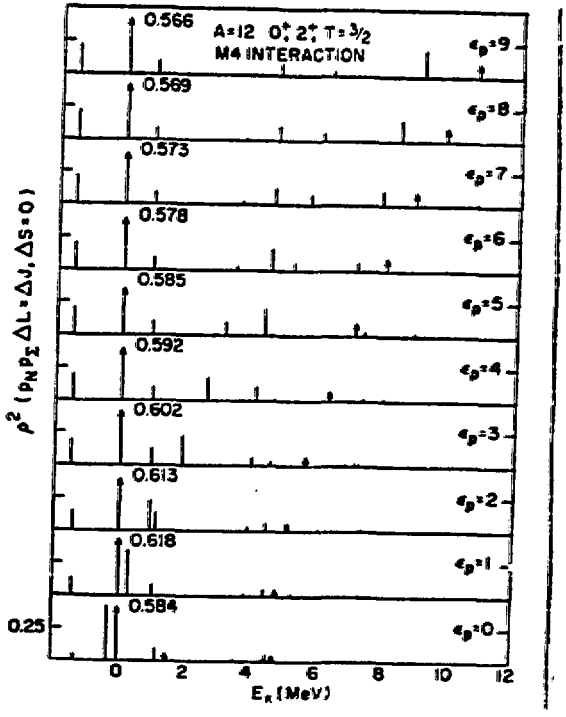

FIGURE 1

Distribution of formation strength, $\rho^2(\Delta S=0)$, as a function of ϵ_p for the M4 interaction. 0^+ states are distinguished by arrowheads.

small energy region as we know experimentally for the Λ hypernuclear case. As ϵ_p increases, and the strength associated with the $p_{1/2}\Sigma$ orbit moves through the spectrum, the possibility of a second peak occurs for ϵ_p = 6 MeV (and maybe a third peak for ϵ_p = 7). However, this interaction does not resemble the model D ΣN interaction and, even for ϵ_p large, tends to concentrate the strength too much in the lowest group of states. In Fig. 2 results for inter-

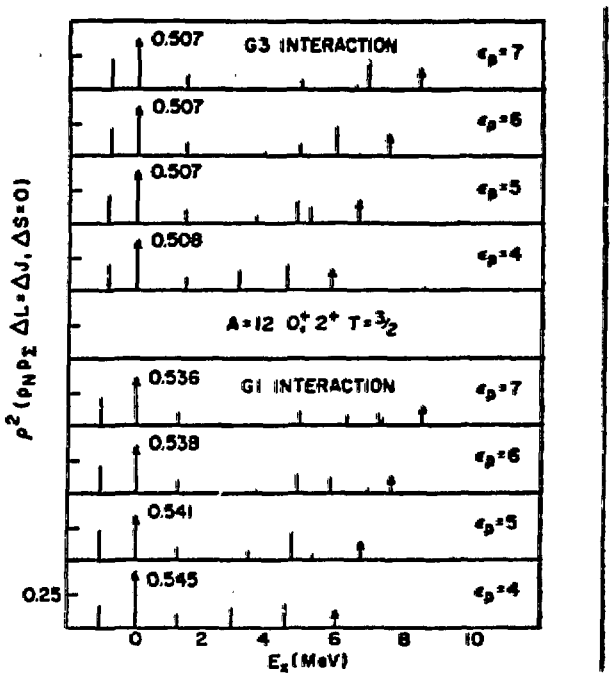

FIGURE 2
Same as Figure 1 for the G1 and G3 interactions.

actions G1 (based closely on model D) and G3 are shown. For ϵ_p = 4 the 2^+ strength is very much spread over the lowest four 2^+ states, but for ϵ_p = 5 the centroid of the 2_3^+, 2_4^+, 2_5^+ group is about 4.7 MeV above that of the 2_1^+, 0_1^+, 2_2^+ group with relative intensities of 31% and 34% for G1 and G3 respectively. However, there is considerable fragmentation, and it is not clear that the KEK data[8] can be convincingly explained by these calculations.

The CERN data[9] for p_K = 450 MeV/c show a single peak in the $^{12}C(K^-,\pi^+)^{12}_{\Sigma}Be$ spectrum at $\Delta M = M_{HY} - M_A$ = 279 MeV and two peaks in the $^{12}C(K^-,\pi^-)^{12}_{\Sigma}C$ spectrum at ΔM = 270 and 275 MeV, while at p_K = 400 MeV/c only the lower of the two peaks appears clearly. The three peaks should correspond to basically $3/2^-$ gs × $p_{3/2}\Sigma$ 0^+ configurations. In order of increasing ΔM denote the states as $|1\rangle$, $|2\rangle$ with T_z = 1/2 and $|3\rangle$ with T_z = − 3/2. Let the T_z = 1/2 states with good isospin be labelled as $|1'\rangle$ and $|2'\rangle$, i.e.,

$$|1'\rangle = |T = 1/2\ T_z = 1/2\rangle = \sqrt{1/3}\,|{}^{11}C \times \Sigma^0\rangle - \sqrt{2/3}\,|{}^{11}B \times \Sigma^+\rangle$$

$$|2'\rangle = |T = 3/2\ T_z = 1/2\rangle = \sqrt{2/3}\,|{}^{11}C \times \Sigma^0\rangle + \sqrt{1/3}\,|{}^{11}B \times \Sigma^+\rangle$$

$$|3\rangle = |T = 3/2\ T = -3/2\rangle = |{}^{11}B \times \Sigma^-\rangle$$

If the strong interaction conserves isospin its contribution, $B_{3/2}$, to the Σ binding energy for states $|2'\rangle$ and $|3\rangle$ is the same. The binding energy, $B_{1/2}$, for state $|1'\rangle$ is in general different from $B_{3/2}$. Dover, Gal and Millener[13] showed that, for any reasonable value of V_c, a value of ΔB not much smaller than E_3-E_1 is required to reproduce the observed separation of states and, furthermore, that the relation

$$E_3-E_2 < 4.93 - 4/3\ V_c\ (\text{MeV})$$

should hold. A consequence of the large value of ΔB is that the isospin mixing in states $|1\rangle$ and $|2\rangle$ is small. If, instead, we start with the charge basis the differences in diagonal energies are

$$E(\Sigma^-) - E(\Sigma^0) = 3.41 - V_c + 1/3\ \Delta B$$

$$E(\Sigma^0) - E(\Sigma^+) = 4.57 - V_c + 1/3\ \Delta B$$

and the off-diagonal matrix element between the Σ^0 and Σ^+ states is $\sqrt{2}\,\Delta B/3$. The large value of ΔB causes considerable mixing and obviously leads to wave functions with close to good isospin. This is evident in the results of the full shell-model calculation presented in Table 4.

Table 4

Interaction V_c(MeV)	M1 2.0	M1 2.85	M3 2.0	M3 2.85
% T = 3/2 in 0_1^+ "T = 1/2"	5.8	3.2	2.0	1.0
% T = 1/2 in 0_2^+ "T = 3/2"	6.1	3.3	2.4	1.1
ΔE ($0_2^+ - 0_1^+$) MeV	4.92	4.37	8.27	7.84
ΔE ($0_3^+ - 0_2^+$) MeV	2.01	1.00	2.15	1.08
ΔE ($0_3^+ - 0_1^+$) MeV	6.9	5.4	10.4	8.9

For the interactions M1, M2, and M3 of Table 3, the force in the two weakest central channels is progressively weakened while maintaining the average values of $F^{(0)}$ for T = 1/2 and T = 3/2; $F^{(0)}_{1/2} = -1.51$ MeV, $F^{(0)}_{3/2} = -0.78$ MeV, $\bar{F}^{(0)} = -1.03$ MeV. Force M1 is similar to that suggested by model D. The three interactions produce almost identical T = 3/2 A=12 spectra. For T = 1/2, however, the lowest 0^+ state becomes progressively more bound. This is equivalent to increasing ΔB. Specifically, for $\epsilon_{p_{3/2}} = 5$ MeV, $V_c = 0$ and mass differences set to zero, the separation between 0_1^+; T = 3/2 and 0_1^+; T = 1/2 are 3.52, 4.91, and 7.13 MeV.

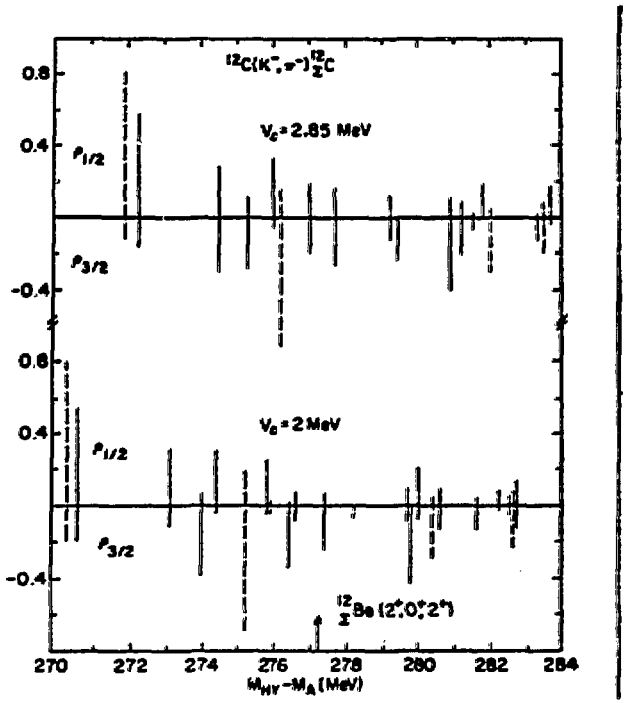

FIGURE 3
ΔS=0 one body density matrix elements for the $^{12}C(K^-,\pi^-)^{12}_{\Sigma}C$ reaction calculated using the Ml interaction. Yamazaki (Ref. 14) has reported peaks at $M_{HY}-M_A$ = 271.2, 277.6 and 282.1 MeV. 0^+ states correspond to dashed lines and 2^+ states to solid lines.

The full distribution of formation strength for $^{12}C(K^-,\pi^-)^{12}_{\Sigma}C$ is shown in Fig. 3 for two values of V_c, where $\rho_{1/2}$ and $\rho_{3/2}$ are the ΔS=0 one-body density matrix elements (not reduced in isospin). Evidently there is, in general, considerable isospin mixing. Also shown are the positions of three peaks reported by Yamazaki at this conference[14]. It may be possible to explain the lowest two peaks, but not the third.

The (K^-,π^+) and (K^-,π^-) formation amplitudes are proportional to $f_L^{(3/2)}(0°)\rho_{3/2}$ and $\sqrt{2/3}\, f_L^{(1/2)}(0°)\rho_{1/2} - \sqrt{1/3}\, f_L^{(3/2)}(0°)\rho_{3/2}$ where $f_L^{(\Delta T)}(0°)$ is the Fermi averaged 0° elementary amplitude. The free space $K^-N\to\pi\Sigma$ lab cross sections at 0° from the analysis of Gopal et al[15] are displayed in Figure 4. They clearly display the effect of Y* resonances, most notably the Y*(1520) at about p_K = 390 MeV/c. Averaging dilutes the effect of the sharp Y* resonances. In Fig. 5 we plot the ratio of cross sections for $^{12}_{\Sigma}C$ (A=11 gs × $p_{3/2}\Sigma$ 0^+ wave functions) for the isospin and charge bases after Fermi-averaging the amplitudes. In the isospin basis the ratio of the two peaks[9] at ΔM=270 and 275 MeV changes more between p_K = 400 and 450 MeV/c than it does in the charge basis. This is the correct trend to explain the data[13]. Detailed comparisons are not possible because cross sections have not been extracted from the data.

2.4 THE A = 16 Σ HYPERNUCLEI

In the case of the $^{16}O(K^-,\pi^+)^{16}_{\Sigma}C$ reaction[10] at p_K = 450 MeV/c the existenc of two peaks about 6.5 MeV apart has been claimed. A spin-orbit splitting of 12 MeV has been deduced[10] in disagreement with the value of 5 MeV claimed fro the $^{12}_{\Sigma}Be$ data[8]. For our ΣN interactions the off-diagonal matrix element, v, between the $p^{-1}_{1/2}N\ p_{1/2}\Sigma$ and $p^{-1}_{3/2}N\ p_{3/2}\Sigma$ 0^+ states is large. For the interaction G1

$$\begin{aligned} v &= P_s + P_t + T \\ -2.57 &= -1.66 + 0.30 - 1.21 \ ; \ T = 1/2 \\ 1.47 &= -0.61 + 1.45 + 0.63 \ ; \ T = 3/2 \ , \end{aligned}$$

where v is broken down into contributions from singlet and triplet central forces and from the tensor force. A consequence of the large v is that the

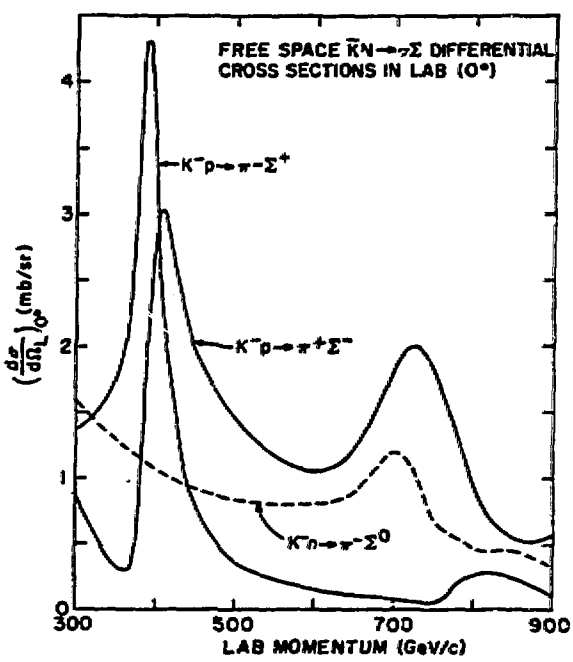

FIGURE 4
Free space $\bar{K}N \to \pi\Sigma$ differential cross sections at 0° as a function of lab K^- momentum.

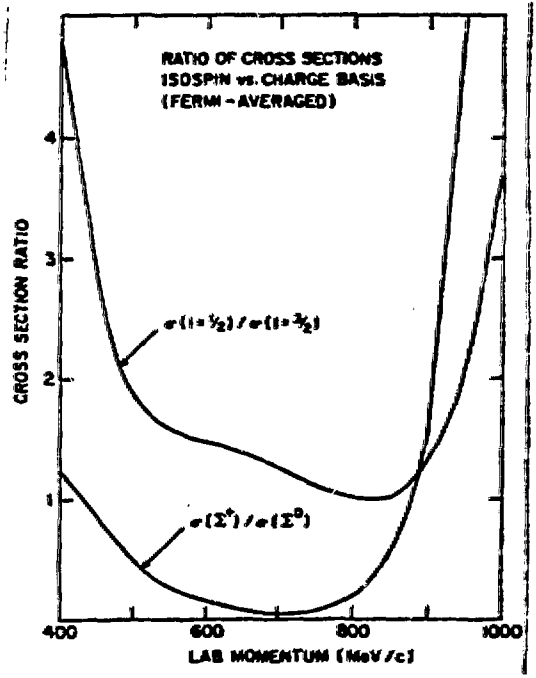

FIGURE 5
Ratio of cross sections for $^{12}_{\Sigma}C$ 0^+ states (see text) in the isospin and charge bases as a function of lab momentum using Fermi-averaged amplitudes.

(K^-,π) formation strength tends to be predominantly in the upper state for T = 3/2 and the lower state for T = 1/2, more or less independently of the spin-orbit splitting. If the two peak structure in $^{16}_{\Sigma}C$ were confirmed it would be a strong indication that the ΣN interaction based on model D is inadequate, as would the empirical need for a large Σ spin-orbit splitting.

3. DISCUSSION

It is clear that we have difficulties in understanding the existing Σ hypernuclear data for A=12 and A=16. In particular, the Σ spin-orbit splitting, ϵ_p, is not unambiguously determined. Such a determination is important in order to differentiate between the predictions of ϵ_p based on one-boson-exchange models[16], and those of quark models[17] inspired by quantum chromodynamics. A number of (K^-,π) experiments better suited than A=12 and A=16 for a determination of ϵ_p have been suggested[12,18,19].

ACKNOWLEDGEMENT. This paper is a report on work done in collaboration with C.B. Dover and A. Gal. This work was supported by the U. S. Department of Energy under contract DE-AC02-76CH00016.

REFERENCES

1. E.H. Auerbach et al, Ann. Phys. (NY) 148 (1983) 381.
2. D.J. Millener, A. Gal, C.B. Dover and R.H. Dalitz, Phys. Rev. C31 (1985) 499.
3. A.R. Bodmer, Q.N. Usmani and J. Carlson, Phys. Rev. C29 (1984) 684.
4. M.M. Nagels, T.A. Rijken and J.J deSwart, Phys. Rev. D12 (1975) 744; 15 (1977) 2547.
5. H. Piekarz et al, Phys. Lett. 110B (1982) 428.
6. R.H. Dalitz and A. Gal, Phys. Lett. 64B (1976) 154.
7. C.J. Batty, Phys. Lett. 87B (1979) 324.
8. T. Yamazaki et al, Phys. Rev. Lett. 54 (1985) 102.
9. R. Bertini et al, Phys. Lett. 136B (1984) 29.
10. R. Bertini et al, Phys. Lett. 158B (1985) 19.
11. C.J. Batty, A. Gal and G. Toker, Nucl. Phys. A402 (1983) 349.
12. A. Gal, this conference.
13. C.B. Dover, A. Gal and D.J. Millener, Phys. Lett 138B (1984) 337.
14. T. Yamazaki, this conference
15. G.P. Gopal et al, Nucl. Phys. B119 (1977) 362.
16. C.B. Dover and A. Gal, Progress in Particle and Nuclear Physics 12 (1984) 171; R. Brockmann, Phys. Lett. 104B (1981) 256; A. Bouyssy, Nucl. Phys. A381 (1982) 445.
17. H.J. Pirner, Phys. Lett. 85B (1979) 190; O Morimatsu, S. Ohta, K. Shimizu and K. Yazaki, Nucl. Phys. A420 (1984) 573.
18. C.B. Dover, A. Gal, L. Klieb and D.J. Millener, BNL preprint
19. J. Zofka, contribution to these Proceedings.